

In situ radiometric mapping as a proxy of sediment contamination: Assessment of the underlying geochemical and -physical principles

E.R. van der Graaf^{a,b,*}, R.L. Koomans^b, J. Limburg^b, K. de Vries^b

^a*Kernfysisch Versneller Instituut, Zernikelaan 25, 9747 AA Groningen, The Netherlands*

^b*MEDUSA Explorations BV, P.O. Box 623, 9700 AP, Groningen, The Netherlands*

Received 19 June 2006; received in revised form 14 November 2006; accepted 19 November 2006

Abstract

Correlations between sediment contaminants like heavy metals or organic micro-compounds and natural or anthropogenic radionuclides (⁴⁰K, ²³⁸U, ²³²Th, ¹³⁷Cs) facilitates in situ mapping of the contaminated sediment using gamma-ray detectors. These maps can be made quickly and economically using surveys with towed underwater gamma-ray detectors and based on the fundamental correlation of contaminants with radioactivity. This paper aims at an assessment of the geochemical and -physical principles underlying these correlations. This assessment uses multivariate analysis of a data base containing information on radionuclides and contaminants for a large number of sediment samples used to derive radionuclide–contaminant correlations in radiometric mapping projects in freshwater bodies of the Netherlands. More specifically, the aims of this study are to test if these correlations are valid for the entire Dutch freshwater environment and to investigate the validity of the thesis that these correlations are mainly due to the presence of clay. © 2006 Elsevier Ltd. All rights reserved.

Keywords: In situ radiometry; Radionuclide; Sediment contamination; Correlations; Multivariate analysis

1. Introduction

Contamination of sediments in lakes, rivers and harbours by heavy metals and organic compounds (including polyaromatic hydrocarbons (PAHs) and PCBs) is an important environmental and economical concern in many countries. Health risks associated with these pollutants may restrict activities like fishing and recreation. Moreover, to maintain access for shipping most waterways and harbours are routinely dredged. An essential waypoint in the management and disposal of such contaminated dredged sediments is their classification on basis of the degree of pollution. Traditionally, inventories of contamination are made using survey programmes with a relatively limited amount of samples and consequently decisions often have to be made on the basis of incomplete information. Because classification of areas as contami-

nated or non-contaminated will often have large financial impact, it is essential that information is both reliable and spatially detailed. Especially the latter aspect is generally not realized in sampling surveys as economical constraints limit the number of samples that are analysed.

This situation can be improved when the environmental parameter to be assessed correlates with a physical parameter that can be measured in situ with a survey device. By establishing the correlation between both parameters on a limited number of samples the in situ survey map of a diagnostic physical parameter can be converted into a quantitative map of the distribution of the environmental parameter.

Concentrations of radionuclides can be measured in situ and can therefore be used as a proxy for contaminants. The MEDUSA method (Koomans and Limburg, 2005; De Meijer et al., 2002) uses the correlation between concentrations of heavy metals and organic micro-contaminants with natural occurring and anthropogenic radionuclides to make synoptic maps of the degree of contamination of extended areas. The MEDUSA method is based on measurements with a gamma-ray scintillation detector that

*Corresponding author. Kernfysisch Versneller Instituut, Zernikelaan 25, 9747 AA Groningen, The Netherlands, Tel.: +31 503 633 562; fax: +31 503 634 003.

E-mail address: vandergraaf@kvi.nl (E.R. van der Graaf).

is towed over the sediment bed behind a vessel. This detection system measures gamma-rays being emitted from very low concentrations of a number of radionuclides (e.g., ^{137}Cs , ^{40}K and radionuclides from the decay series of ^{238}U and ^{232}Th) in sediment. Typically, the system needs 1–10 s to accumulate sufficient data such that the gamma-ray spectrum can be decomposed into the contribution of the individual radionuclides. Consequently, the sediment bed can be probed at a few hundred to a few thousand locations per hour. Due to the attenuation of gamma radiation in the sediment the concentrations measured by MEDUSA are characteristic for the top 30–50 cm of the sediment bed.

As an example we show (Fig. 1) the correlation between a heavy metal (Ni) with ^{238}U in sediments from Dutch rivers (Meuse and Rhine). This correlation is derived from measurements (heavy metals: ICP-MS; radionuclides: gamma spectrometry) on 50 sediment samples taken from these rivers. This correlation has been used to map the Ni distribution in these rivers by converting radionuclide concentration maps of the river bottom that were measured with the MEDUSA detector for underwater bottom gamma-ray activity (Fig. 2). The size of the survey area was approximately 60 km² and has been mapped within 10 working days.

The example shows that in case a correlation exists between the concentration of a radionuclide and a parameter quantifying environmental pollution, maps can be composed that contain information that is far more detailed than any map that is based on interpolation of a limited number of sampling locations.

The MEDUSA method has been applied in a multitude of projects and in most instances quantitative correlations could be derived to convert radionuclide concentrations into information on relevant environmental parameters.

In previous projects the correlations were all derived empirically and applied as a conversion tool. The

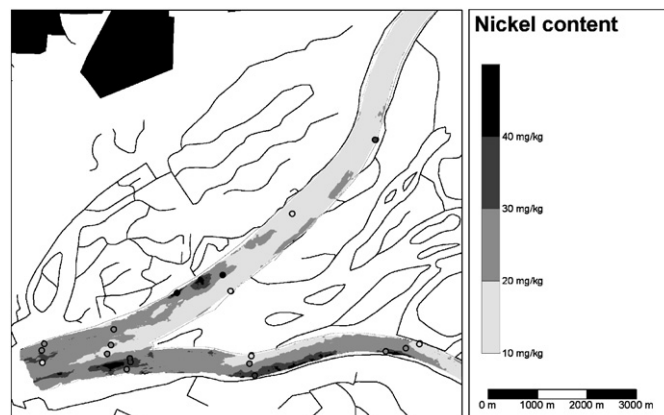


Fig. 2. Map of Ni distribution in Meuse and Rhine sediments.

geochemical and -physical foundation of the correlations has not been considered in detail before and is topic of this paper. Improved knowledge of the processes underlying the correlations between radionuclides, heavy metals and organic micro-contaminants will enable a better estimate of the scope of the method.

In this paper, these correlations will be assessed by combining information from literature on geochemical and -physical properties of the relevant radionuclides and environmental parameters with information from the project database of MEDUSA Explorations BV that is filled with radiometric data (measured by MEDUSA) and data on sediment contaminants and grain-sizes (measured by specialized laboratories). As most of the information in the database relates to freshwater studies in the Netherlands we will focus on sediments from the Dutch freshwater environment.

The main objectives of this study are:

1. Correlations between contaminants and radionuclides have been found in projects that each represent part of the Dutch freshwater environment. It is an open question if some of the correlations will hold up for the entire Dutch freshwater environment. This question will be addressed in this study.
2. At the moment, the correlations between contaminants and radionuclides are thought to be brought about mainly due to the presence of clay containing higher concentrations of radionuclides in combination with it also having a higher affinity for contaminants. This study will investigate the validity of this hypothesis.

1.1. The freshwater environment in The Netherlands

The Dutch freshwaters can be divided into lakes, rivers and canals. Sediment samples of all these different settings are present in the MEDUSA database. Typical ranges for concentrations of pollutants in sediments in moderately to extremely contaminated areas in the Netherlands are given in Table 1 together with maximum allowable concentrations and concentrations at which the risk is considered

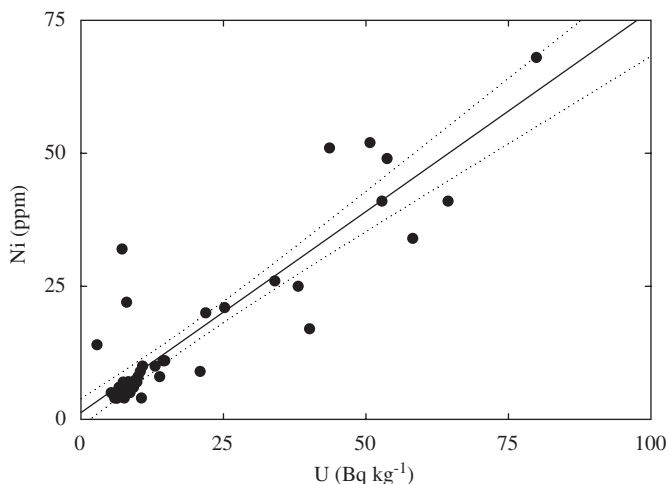


Fig. 1. Correlation between Ni and ^{238}U in Meuse and Rhine sediments. Solid line is linear regression $\text{Ni (ppm)} = 1.26 + 0.76\text{U (Bq kg}^{-1}\text{)}$ ($R^2 = 0.82$). Dotted lines are 95% confidence intervals.

Table 1
Ranges for heavy metals and polyaromatic hydrocarbons (PAH) in Dutch freshwaters sediments

Contaminant	Range (ppm)	NR (ppm) ^a	MAC (ppm) ^a
Ni	10–120	35	44
Zn	100–1700	140	620
Cd	1–50	0.8	12
Cu	20–280	36	73
Pb	20–240	85	530
Hg	0.4–5	0.3	10
Cr	20–290	100	380
As	4–50	29	55
PAH	0.02–100	0.3	34

Concentrations (NR) at which the risk is considered negligible and maximum allowable concentrations (MAC) are also presented.

Table based on data from: Van den Berg et al. (1999), Lahr et al. (2003), Winkels et al. (1998), Römken et al. (2003), Struijs et al. (2000), NW4 (1999) and MNP (2006).

PAH: Total amount of ten selected polyaromatic hydrocarbons: naphthalene, phenanthrene, anthracene, fluoranthene, benzo(a)anthracene, chrysene, benzo(k)fluoranthene, benzo(a)pyrene, benzo(ghi)perylene, indeno (123-cd)pyrene.

^aValues are normalised to a standard sediment with 10% organic matter and 25% lutum (<2 mm) contents.

negligible (background values) according to Dutch standards (NW4, 1999).

The freshwater sediments are mainly a mixture of sand, clay, and organic materials in the case of rivers and canals, for the lakes, the sediments usually contain a much higher organic fraction. The sand fraction is essentially quartz with feldspar (5–20%) and some mica (1–5%). The clay fraction of the large river sediments (Rhine, Meuse) comprises mainly the clay minerals illite (30–40%), smectite (10–35%), vermiculite (5–20%), kaolinite (5–10%) and chlorite (5–10%). For other rivers the composition may be different, e.g. for the smaller river IJssel, the clay fraction consists largely of smectite (50–80%) with some kaolinite and chlorite (Locher and De Bakker, 1990).

1.2. Radionuclides in the Dutch freshwater sediments

1.2.1. Uranium

Uranium occurs naturally in trace amounts in sediments by its incorporation in clay, sand and in some heavy minerals. In the Netherlands typical concentrations in clays (45 Bq kg⁻¹) are higher than in sand (5 Bq kg⁻¹). In heavy minerals, much higher concentrations can be found (in zircon several kBq kg⁻¹; Mohanty et al., 2004). Some relatively small amounts of anthropogenic uranium are released by the phosphate and fertilizer industry. However, locally these discharges may lead to enhanced uranium concentrations.

1.2.2. Thorium

Thorium is also naturally present in sediments in approximately similar concentrations in clay and sand as

uranium. In heavy minerals high concentrations can be found (more than 100 kBq kg⁻¹ in the case of monazite; Mohanty et al., 2004). Some very small amounts of thorium are discharged by the Dutch phosphate and fertilizer industry that nevertheless might lead to locally enhanced concentrations.

1.2.3. Potassium

Potassium constitutes about 2.4% of the mass of the Earth and is present at %-level in clays, feldspars and mica's. The natural radioisotope ⁴⁰K has an abundance of 0.0119% leading to an activity concentration of approximately 200 Bq kg⁻¹ in sand and 700 Bq kg⁻¹ in Dutch clays (Venema and De Meijer, 2001).

1.2.4. Caesium

There is a distinct difference between the natural radionuclides and ¹³⁷Cs in the way they are distributed in a sediment bed. The natural radionuclides will at least initially be a more or less integral part of the minerals comprising the sediment while ¹³⁷Cs is a later surface addition that has been distributed in the environment by atmospheric testing of nuclear weapons in the 1960s and by the Chernobyl accident. Furthermore, ¹³⁷Cs fall-out from the testing might be considered to be homogeneously distributed while, in contrast, the ¹³⁷Cs from Chernobyl has been preferentially deposited along a 150 km broad strip in northwest–southeast direction passing over the centre of the Netherlands.

1.3. MEDUSA project data base

The MEDUSA project data base contains information on more than a 1000 sediment samples from projects from 1996 up to present. For this study, only samples taken in the Dutch freshwater environment were used and from these a selection was made of samples of which information was available on concentrations of radionuclides, heavy metals and organic micro-compounds. This resulted in a subset of 13 projects comprising 232 samples. In Fig. 3 the locations of the projects are indicated on a map of the Netherlands. Table 2 presents an overview of the descriptive statistics of the selected samples.

2. Materials and methods

2.1. Metals, PAHs, grain size analysis and radiometry

Samples were obtained with a boxcorer or a multi-sampler. After sampling, the sediments were stored in glass containers and cooled prior to analysis in the laboratory. The heavy metal concentrations (As, Cr, Cu, Pb, Ni, Zn, Hg, Cd), concentrations of PAHs and the grain size distributions are determined with standard procedures by XRF, ICP and GCMS methods by three specialized Dutch laboratories (Alwest Laboratories, Deventer, The Netherlands, Alcontrol Laboratories BV, Hoogvliet,



Fig. 3. Map of the Netherlands with the location of the projects indicated by dots.

Table 2
Descriptive statistics of the selected samples: complete data set

Parameter	Mean \pm SEM (<i>n</i>)	Range
^{40}K (Bq kg $^{-1}$)	345 \pm 8 (232)	60–780
^{238}U (Bq kg $^{-1}$)	22.0 \pm 0.7 (232)	3–80
^{232}Th (Bq kg $^{-1}$)	19.4 \pm 0.6 (232)	5–53
^{137}Cs (Bq kg $^{-1}$)	9.3 \pm 0.7 (232)	0–72
Pb (ppm)	66 \pm 7 (226)	11–1100
Zn (ppm)	208 \pm 15 (209)	20–1600
Ni (ppm)	16.3 \pm 0.7 (226)	4–68
Cd (ppm)	2.4 \pm 0.4 (232)	0.1–57
Cu (ppm)	36 \pm 3 (226)	3–320
Cr (ppm)	32 \pm 3 (216)	6–540
Hg (ppm)	1.2 \pm 0.3 (230)	0.05–37
As (ppm)	9.5 \pm 0.4 (207)	2–61
PAH (ppm)	7.4 \pm 0.7 (225)	0.02–83
TOC (%)	10.2 \pm 0.7 (232)	0.5–68
Grain size < 16 μm (%)	19.2 \pm 1.3 (225)	0–97
Grain size < 63 μm (%)	38 \pm 2 (211)	0.5–99

TOC: total organic content. PAH: see Table 1.

The Netherlands and Analytico Milieu BV, Barneveld, The Netherlands). The concentrations of ^{238}U , ^{232}Th , ^{40}K and ^{137}Cs are determined with a low-background gamma spectrometer consisting of a CsI scintillation detector placed in a lead castle with 10 cm thick walls. Spectra were analysed using full spectrum analysis (Hendriks et al., 2001). Calibrated standard spectra were obtained by

measurements of certified reference materials in identical containers as were used for the sample measurements.

2.2. Multivariate analysis

In this study, SPSS for windows (version 13.0.1) was used for correlation analysis and for principal component (PCA) and cluster analysis (CA). These methods are used frequently in studies that involve large data sets with many parameters per sample (Lee et al., 2006; Golobočanin et al., 2004; Sena et al., 2002). In correlation analysis the correlation coefficients between the variables are calculated to determine their mutual relationships. PCA reduces data by combining a number of the (possibly correlated) original variables in a set of new uncorrelated variables (the principle components) that are ordered in their contribution in explaining the data sets variation. CA can be applied to classify variables that are similar in groups.

3. Results

3.1. Assessment and transformation of distributions

Geochemical and environmental data is often not normally distributed (Reimann and Filzmoser, 1999). As multivariate analysis is sensitive to this non-normality it is important to assess the distribution of the original data. Commonly data sets are positively skewed (asymmetric with a tail towards positive values) and may have high kurtosis values (more 'peaked' than a normal distribution). Our data set also exhibits these distributions for most of the variables (Table 3). Kolmogorov–Smirnov tests (Miller and Miller, 2005) for normality showed that only the distribution of U could be considered normal (Kolmogorov–Smirnov $p > 0.05$). Furthermore, it appeared that both the distributions of Th and K were bimodal (Fig. 4). This is most prominent in the distribution of Th where a natural division seems apparent at a Th concentration of 20 Bq kg $^{-1}$. To assess possible effects of the bi-modality the data set was split into two subgroups, one containing only samples with a Th activity concentration less than 20 Bq kg $^{-1}$ (group Th < 20) and one with concentrations higher than 20 Bq kg $^{-1}$ (group Th > 20). This division rendered both the distributions of Th and K unimodal (Fig. 4). The descriptive statistics of the two subgroups in Table 4 show that for all radionuclides and for almost all metals the concentrations in the Th < 20 group are significantly lower than in the Th > 20 group, only Pb and Cd are exceptions. The concentrations TOC and PAH are not significantly different between the two subgroups. The percentage of small size grains in the Th > 20 group is approximately a factor of 4 higher compared to the Th < 20 group.

The division of our data set into two subgroups improved the normality of the distribution of the variables, especially so for K and Th. However, the majority of the variables are still not normally distributed (Table 3).

Table 3
Distribution variables skewness (*S*) and kurtosis (*K*) and Kolmogorov–Smirnov *p*-value for normality tests

Parameter	All data			Th<20			Th>20		
	<i>S</i>	<i>K</i>	<i>p</i>	<i>S</i>	<i>K</i>	<i>p</i>	<i>S</i>	<i>K</i>	<i>p</i>
⁴⁰ K	0.45	-0.39	0.02	0.15	0.221	0.77	0.06	1.07	0.49
²³⁸ U	1.23	3.33	0.12	-0.06	-0.93	0.15	2.16	6.97	0.00
²³² Th	0.62	-0.44	0.00	0.00	-1.11	0.27	1.14	2.56	0.41
¹³⁷ Cs	2.31	7.89	0.00	1.92	4.08	0.00	1.98	5.45	0.03
Pb	6.39	53.1	0.00	6.33	46.9	0.00	2.69	8.58	0.00
Zn	2.92	11.7	0.00	4.05	24.0	0.00	2.23	6.93	0.00
Ni	1.73	4.00	0.00	2.93	11.6	0.00	1.80	4.22	0.01
Cd	5.92	43.8	0.00	6.34	48.3	0.00	4.30	19.9	0.00
Cu	3.24	13.2	0.00	3.46	15.3	0.00	2.91	10.5	0.00
Cr	7.36	71.2	0.00	5.90	47.2	0.00	5.36	34.5	0.00
Hg	6.30	44.6	0.00	6.85	58.3	0.00	3.95	16.9	0.00
As	3.36	16.7	0.00	4.68	29.8	0.00	3.02	13.3	0.00
PAH	3.36	16.3	0.00	3.51	16.3	0.00	1.87	3.23	0.00
TOC	2.46	7.23	0.00	2.51	6.57	0.00	2.37	8.47	0.01
<16 μm	1.16	0.62	0.00	4.48	29.9	0.00	0.02	-0.69	0.77
<63 μm	0.49	-1.09	0.00	1.49	2.24	0.07	-0.40	-0.57	0.55

Original data.

To improve the normality all distributions were transformed using the Box–Cox transformation (Meloun et al., 2005) and again assessed for skewness, kurtosis and normality. The transformed data showed much smaller values for skewness and kurtosis (Table 5) indicating more symmetrically distributed data and moreover the number of variables that passed the Kolmogorov–Smirnov test increased significantly. Consequently, in the next steps of the data analysis the Box–Cox transformed distributions were used to suppress biasing and other effects due to deviations from normality.

3.2. Correlation analysis

The Pearson correlation coefficients between the four radionuclides, the grain size fraction smaller than 63 μm and all other variables (Fig. 5) indicate that K, U and Th positively correlate with each other. In addition, strong positive correlations are found between U and Cs and the other variables, especially with the metals. All four radionuclides also positively correlate with the grain size fractions smaller than 16 and 63 μm.

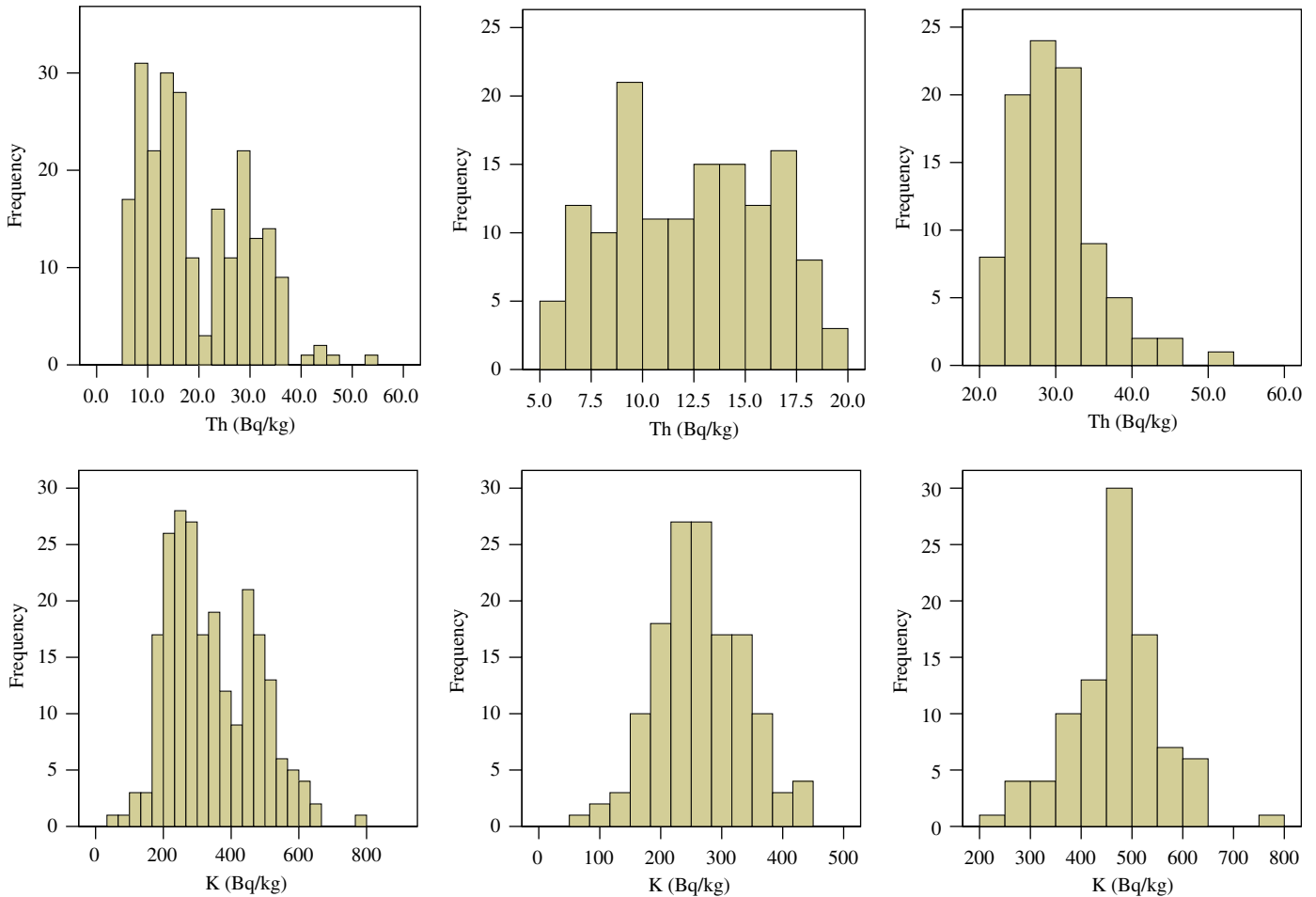


Fig. 4. Distributions of Th (top) and K (bottom). Presented from left to right are all data, data from Th<20 group and data from Th>20 group.

Table 4
Descriptive statistics of the two subsets of the selected samples

Parameter	Th < 20		Th > 20	
	Mean ± SEM (n)	Range	Mean ± SEM (n)	Range
⁴⁰ K (Bq kg ⁻¹)	264 ± 6 (139)	60–450	469 ± 10 (93)	219–780
²³⁸ U (Bq kg ⁻¹)	15.1 ± 0.5 (139)	3–30	32.2 ± 1.0 (93)	19–80
²³² Th (Bq kg ⁻¹)	12.3 ± 0.3 (139)	5–20	30.0 ± 0.6 (93)	20–53
¹³⁷ Cs (Bq kg ⁻¹)	6.0 ± 0.6 (138)	0–38	14.1 ± 1.3 (98)	0.4–72
Pb (ppm)	66 ± 10 (139)	11–1100	67 ± 7 (87)	13–400
Zn (ppm)	140 ± 13 (118)	20–1200	284 ± 27 (91)	20–1600
Ni (ppm)	11.8 ± 0.8 (139)	4–67	23.5 ± 1.1 (87)	7–68
Cd (ppm)	2.5 ± 0.5 (139)	0.1–57	2.3 ± 0.5 (87)	0.2–32
Cu (ppm)	31 ± 3 (139)	3–270	44 ± 6 (87)	5–320
Cr (ppm)	19.1 ± 1.4 (137)	6–170	54 ± 8 (79)	15–540
Hg (ppm)	0.26 ± 0.04 (137)	0.05–4.5	2.6 ± 0.6 (93)	0.05–37
As (ppm)	7.4 ± 0.6 (120)	2–61	12.4 ± 0.8 (87)	4–55
PAH (ppm)	7.5 ± 1.0 (139)	0.02–83	7.3 ± 0.8 (86)	0.1–37
TOC (%)	9.3 ± 1.1 (139)	0.5–68	11.6 ± 0.8 (93)	1–54
Grain size < 16 μm (%)	8.1 ± 1.0 (138)	0–97	36.7 ± 1.9 (87)	1–78
Grain size < 63 μm (%)	18.1 ± 1.5 (124)	0.5–78	66 ± 2 (87)	5–99

Table 5
Distribution variables skewness (*S*) and kurtosis (*K*) and Kolmogorov–Smirnov *p*-value for normality tests

Parameter	All data			Th < 20			Th > 20		
	<i>S</i>	<i>K</i>	<i>p</i>	<i>S</i>	<i>K</i>	<i>p</i>	<i>S</i>	<i>K</i>	<i>p</i>
⁴⁰ K	-0.32	0.12	0.14	-0.82	2.19	0.71	-0.58	1.24	0.16
²³⁸ U	1.23	3.34	0.12	-0.50	-0.65	0.04	1.36	3.13	0.03
²³² Th	0.02	-1.05	0.05	-0.24	-0.99	0.35	0.77	1.33	0.65
¹³⁷ Cs	-0.78	-0.25	0.00	-0.53	-0.51	0.70	-1.18	1.09	0.02
Pb	0.61	0.35	0.05	0.73	0.59	0.02	0.48	-0.07	0.24
Zn	0.06	-0.13	0.93	0.24	0.23	0.84	-0.29	0.08	0.50
Ni	0.30	-0.42	0.53	1.18	1.77	0.05	0.61	1.01	0.28
Cd	0.05	0.08	0.00	0.13	-0.14	0.00	0.06	0.28	0.10
Cu	0.20	-0.34	0.31	0.20	-0.48	0.09	0.40	-0.27	0.25
Cr	1.10	2.24	0.00	1.76	5.94	0.00	1.20	2.76	0.04
Hg	0.90	0.57	0.00	0.60	0.05	0.00	0.23	-0.08	0.76
As	0.73	0.73	0.00	1.51	3.36	0.00	0.78	1.95	0.13
PAH	-0.82	1.52	0.03	-0.74	1.52	0.05	-0.76	0.62	0.13
TOC	-0.70	-0.01	0.00	-0.46	-0.77	0.01	0.08	0.92	0.65
< 16 μm	-0.90	-0.18	0.01	-0.53	-0.75	0.01	-2.26	7.62	0.01
< 63 μm	-1.53	1.91	0.00	-1.19	0.66	0.00	-2.16	8.33	0.09

Box–Cox transformed data.

Table 6 that presents all correlations in numerical form shows that also strong correlation exists between the metals, e.g. Cu positively correlates with both Pb and Zn and Cr correlates with Ni.

3.3. Principal component analysis

PCA was used on all data and the two subgroups (Th < 20 and Th > 20) to identify relationships between the various variables. In this analysis the number of components to be extracted was based on a Scree test (Zhu and Ghodsi, 2006), keeping only components with eigenvalues larger than one.

The loadings of the principal components were rotated for maximum variance (Dyrstad, 1998) (Table 7).

In all three cases four components were extracted. The total variance explained ranged from 79% to 83%. Principal component 1 (PC1) contains Pb, Zn, Cu and Cd (although the loading is slightly less than 0.7 for all data) in case for all data and the two subgroups. For all data and group Th < 20 PAH also has a high loading in PC1 while in addition in the Th < 20 group ¹³⁷Cs is significantly present. The situation for PC1 in subgroup Th > 20 is rather different as here all metals (except for Hg) and ²³⁸U are dominant. It appears that in this latter subgroup the metals Ni and Cr have moved from PC3 towards PC1.

For all data the three natural radionuclides dominate one principal component (PC2), in contrast, in the group Th < 20 ⁴⁰K is very strong in PC4 whilst ²³⁸U and ²³²Th seem to have been distributed between PC2 and PC4. In the group Th > 20 ⁴⁰K and ²³²Th are together in PC2 but ²³⁸U is strongly present in PC1 and seems to be associated with the metals (excluding Hg and not as clear for As).

The grain size indicators and TOC make up one component in all data (PC4) and in the group Th < 20 (PC2) and also dominate in PC4 in the group Th > 20 although some of the loading of the grain size indicators seems to have moved to PC2 in which ⁴⁰K and ²³²Th have high loadings.

Hg appears to differ from the other metals, it only has a significant loading in PC3 of the group Th > 20 in which it is associated with PAH.

3.4. Cluster analysis

Hierarchical CA was used to identify groups of similar variables. In the CA Ward's method was combined with

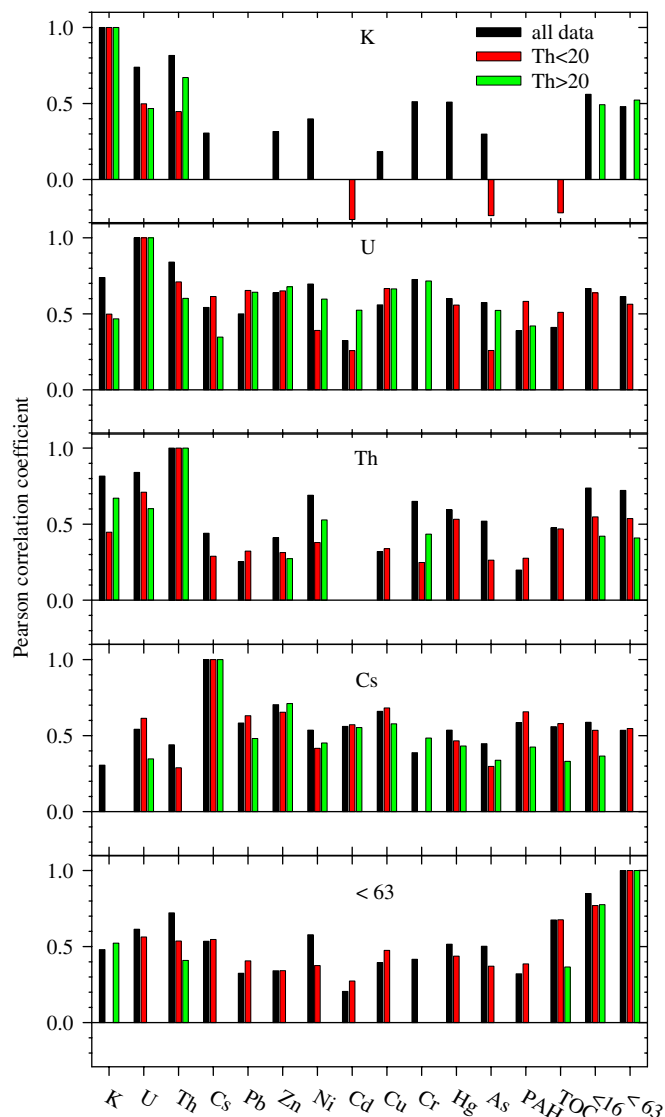


Fig. 5. Pearson correlation coefficients of radionuclides K, U, Th, Cs and grain size percentage $<63 \mu\text{m}$ with all variables. Only correlations that are significant at $p < 0.01$ (two-sided) are shown.

squared Euclidian distance and standardization of the data to the z -score was applied.

The dendrogram resulting from the CA for all data shows the variables Cu, Pb, Zn Cd and PAH as a distinct group. This is consistent with the PCA where these variables are present in PC1 with high loadings. The other variables may be classified into three other clusters namely, a cluster with Cr, Ni As and Hg, a cluster with K, U and Th and finally a cluster with Cs, TOC and the grain sizes. Except for Hg and Cs, these clusters are consistent with the loadings of PC3, PC2 and PC4, respectively.

Also the CA for the group Th <20 reflects the loadings of the PCA. K forms a cluster by itself (conform its high loading in PC4), TOC and the grain sizes are in one cluster (PC2) and the remaining two clusters can be associated with PC1 (Cu, Pb, Zn, Cd, Cs, U and PAH) and PC3 (Cr, Ni, Th, Hg and As). In the association to the latter two

clusters, the position of U and Th is not entirely consistent with the PCA, probably reflecting the fact that both radionuclides had relatively high loadings in more than one PC.

For the group Th >20 the dendrogram for CA also shows similarity with the PCA results. The radionuclides Th and K scoring high in PC2 are combined in one cluster and seem to be associated with the grain sizes that also have relatively high loadings in PC2. The metals Cu, Zn, Pb and Cd are very closely associated and also to a somewhat lesser degree to Cs, PAH, Cr, Ni, U and As. All of these parameters (only PAH is an exception) also have high loadings in PC1. The components PC3 and PC4 are not clearly reflected in the CA, that actually only reveals two clusters and the variables that have high loadings in these components appear to be mixed amongst these two clusters (Fig. 6).

4. Discussion

The mean concentrations and ranges of the natural radionuclides ^{40}K , ^{238}U and ^{232}Th (Table 2) are representative for Dutch freshwater sediments (Van Wijngaarden et al., 2002). The mean ^{137}Cs concentration is similar to those found in other European freshwater sediments (e.g., $8.8 \pm 1.5 \text{ Bq kg}^{-1}$ in Danube sediments; Bikit et al., 2006). The mean contents of metals and PAHs are somewhat lower than those found in sediments of inner city canals (Kelderman et al., 2000). Using the mean values of Hg, PAH and Cd as a criterion the sediments would be classified slightly polluted according to the Dutch system of sediment pollution assessment. For all metals (except Ni) and for PAH the upper bound of their range (Table 2) would classify the sediments as very polluted, indicating that the data set as a whole covers a broad range of possible degrees of contamination.

The division of the data set using the, in a way rather arbitrary, boundary criterion $\text{Th} = 20 \text{ Bq kg}^{-1}$ resulted into two subgroups where for almost all parameters the concentrations in the Th >20 group were higher than in the Th <20 group. Especially noteworthy is the fact that fraction of grain sizes <63 and $<16 \mu\text{m}$ in the Th >20 group is much larger than in the Th <20 group. To explore this somewhat further the relation between the ^{232}Th concentration and the percentage of grain sizes $<63 \mu\text{m}$ is presented in Fig. 7. This figure shows that the $\text{Th} = 20 \text{ Bq kg}^{-1}$ level (dotted line, Fig. 7) splits the data set quite naturally in a group with sandy samples (fraction $<63 \mu\text{m}$ between 0% and 40–50%) and a group with clayey samples (fraction $<63 \mu\text{m}$ between 40–50% and 100%). The entire data set shows an approximate linear relation ($R^2 = 0.72$) between ^{232}Th and the fraction $<63 \mu\text{m}$.

The activity concentrations of ^{238}U and ^{40}K are about a factor 2 higher in the Th >20 group compared to the Th <20 group. Clay having higher contents of natural radionuclides than sand indicates consistency with the

Table 6

Pearson correlation coefficients of metals and other variables for all data (upper part of table) and for the Th < 20 and Th > 20 groups (lower part of the table)

All data																
	⁴⁰ K	²³⁸ U	²³² Th	¹³⁷ Cs	Pb	Zn	Ni	Cd	Cu	Cr	Hg	As	PAH	TOC	<16	<63
	0.739															
	0.816	0.840														
	0.306	0.542	0.440													
	n.s.	0.500	0.254	0.583												
	0.316	0.639	0.411	0.704	0.771											
	0.399	0.696	0.690	0.536	0.456	0.663										
	n.s.	0.324	n.s.	0.561	0.654	0.647	0.473									
	0.184	0.559	0.320	0.660	0.841	0.823	0.582	0.656								
	0.512	0.726	0.650	0.388	0.357	0.639	0.819	0.327	0.445							
	0.509	0.600	0.594	0.536	0.472	0.590	0.567	0.349	0.488	0.640						
	0.299	0.574	0.520	0.447	0.452	0.567	0.692	0.422	0.471	0.670	0.592					
	n.s.	0.389	0.198	0.586	0.660	0.597	0.279	0.397	0.713	n.s.	0.381	0.300				
	n.s.	0.411	0.476	0.559	0.441	0.380	0.649	0.368	0.521	0.351	0.471	0.534	0.381			
	0.561	0.666	0.738	0.588	0.369	0.447	0.647	n.s.	0.470	0.479	0.580	0.460	0.414	0.703		
	0.480	0.614	0.722	0.535	0.325	0.341	0.578	0.205	0.395	0.417	0.516	0.502	0.321	0.675	0.849	
Th < 20																
	⁴⁰ K	²³⁸ U	²³² Th	¹³⁷ Cs	Pb	Zn	Ni	Cd	Cu	Cr	Hg	As	PAH	TOC	<16	<63
	0.467	0.671	n.s.	n.s.	n.s.	n.s.	n.s.	n.s.	n.s.	n.s.	n.s.	n.s.	n.s.	n.s.	0.492	0.523
	0.498	0.602	0.347	0.642	0.678	0.597	0.524	0.664	0.716	n.s.	0.523	0.420	n.s.	n.s.	n.s.	n.s.
	0.447	0.710	n.s.	n.s.	0.273	0.528	n.s.	n.s.	0.434	n.s.	n.s.	n.s.	n.s.	n.s.	0.421	0.409
	n.s.	0.614	0.289	0.481	0.711	0.452	0.553	0.578	0.484	0.432	0.338	0.425	0.331	0.366	n.s.	n.s.
	n.s.	0.654	0.323	0.631	0.858	0.593	0.708	0.847	0.669	0.504	0.444	0.551	n.s.	n.s.	n.s.	n.s.
	n.s.	0.651	0.313	0.654	0.749	0.700	0.774	0.856	0.771	0.443	0.549	0.605	n.s.	n.s.	n.s.	n.s.
	n.s.	0.391	0.379	0.417	0.435	0.627	0.719	0.645	0.881	n.s.	0.560	n.s.	0.405	0.298	n.s.	n.s.
	-0.263	0.258	n.s.	0.572	0.624	0.624	0.432	0.742	0.665	0.411	0.482	0.321	n.s.	n.s.	n.s.	n.s.
	n.s.	0.666	0.339	0.682	0.837	0.811	0.577	0.613	0.731	0.411	0.434	0.593	n.s.	n.s.	n.s.	n.s.
	n.s.	0.189	0.248	n.s.	n.s.	0.454	0.667	n.s.	0.402	0.740	0.419	n.s.	n.s.	n.s.	n.s.	n.s.
	0.198	0.558	0.532	0.466	0.542	0.648	0.498	0.337	0.583	0.523	0.506	0.409	0.277	0.400	n.s.	n.s.
	-0.237	0.259	0.263	0.298	0.417	0.486	0.594	0.337	0.422	0.417	0.434	0.338	n.s.	0.311	n.s.	n.s.
	n.s.	0.582	0.276	0.657	0.701	0.602	0.293	0.417	0.763	n.s.	0.426	n.s.	n.s.	n.s.	n.s.	n.s.
	-0.219	0.510	0.469	0.579	0.530	0.417	0.633	0.410	0.623	n.s.	0.523	0.525	0.481	0.485	0.366	0.776
	n.s.	0.638	0.548	0.535	0.449	0.432	0.467	n.s.	0.566	n.s.	0.462	n.s.	0.506	0.712	0.776	0.776
	n.s.	0.563	0.537	0.547	0.406	0.342	0.375	0.274	0.475	n.s.	0.437	0.371	0.386	0.676	0.770	0.770
Th > 20																

Only correlations that are significant at $p < 0.01$ (two-sided) are presented.

n.s.: not significant.

interpretation that the former group represents clayey samples while the latter comprises sandy samples.

4.1. Correlations

Before commencing a detailed discussion on the underlying mechanisms that may lead to correlations it is important to firstly emphasize the fact that for these correlations to be useful in contamination mapping the levels of the contaminant should be clearly above the variability in the 'natural background levels'. In most of the projects in the MEDUSA data base a sizable fraction of the samples only represents uncontaminated levels. This is nicely illustrated by the cloud of data points in the lower left corner of Fig. 1 where the majority of the measurements show low Ni and U concentrations representing 'natural background levels'. It is the presence of the data with clearly higher concentrations that defines the correlation.

Correlations between two compounds in freshwater sediment may come about by a more or less similar fate

of these compounds. This fate is determined by both transport and interaction processes of the compounds in/with the materials of the freshwater environment. Consequently, correlations in sediments between environmental parameters like heavy metals and PAH and radionuclides will be induced by interactions with the sediment that result in high or low concentrations at the same position in the sediment bed.

Starting from a *dispersed* contamination, concentration variations may be induced by local differences in sediment properties leading to different interactions, i.e. absorption to clay or by physical selection processes, i.e. settling at the inner bend of a river bed due to velocity differences. In case both a contaminant and a radionuclide can be assumed to be dispersedly present and similar affected by transport and interaction processes, correlation between the contaminant and the radionuclide may be expected.

Alternatively, correlations with radionuclides may also originate from the presence of radionuclides being indicative for properties of the sediment. For example, the fact that a high natural radionuclide content in sediment is a

Table 7
Principal component loadings from PCA on all data, and the data from the Th < 20 and Th > 20 subgroups

Par.	All data				Group Th < 20				Group Th > 20			
	PC1	PC2	PC3	PC4	PC1	PC2	PC3	PC4	PC1	PC2	PC3	PC4
⁴⁰ K	0.03	0.95	0.14	0.07	0.03	−0.06	−0.10	0.94	0.02	0.93	0.11	−0.11
²³⁸ U	0.38	0.74	0.31	0.34	0.52	0.48	0.17	0.58	0.74	0.48	0.14	−0.27
²³² Th	0.05	0.77	0.37	0.42	0.04	0.61	0.29	0.59	0.42	0.76	−0.27	0.07
¹³⁷ Cs	0.67	0.24	0.18	0.41	0.74	0.41	0.07	0.03	0.54	−0.05	0.42	0.31
Pb	0.86	0.07	0.23	0.13	0.84	0.23	0.20	0.09	0.79	−0.02	0.42	−0.05
Zn	0.77	0.26	0.48	0.03	0.78	0.09	0.50	0.19	0.86	0.03	0.41	0.02
Ni	0.27	0.28	0.74	0.41	0.30	0.33	0.77	−0.10	0.88	0.17	−0.14	0.33
Cd	0.69	−0.22	0.45	0.08	0.77	0.00	0.23	−0.34	0.87	−0.13	0.12	0.08
Cu	0.86	0.12	0.27	0.21	0.83	0.31	0.26	0.09	0.84	−0.01	0.36	−0.04
Cr	0.17	0.45	0.81	0.07	0.00	−0.05	0.92	0.13	0.85	0.27	0.15	0.13
Hg	0.35	0.46	0.47	0.25	0.40	0.30	0.57	0.32	0.26	0.09	0.72	0.32
As	0.25	0.16	0.73	0.32	0.23	0.29	0.65	−0.24	0.57	0.25	0.29	0.17
PAH	0.83	0.18	−0.15	0.22	0.80	0.30	−0.08	0.17	0.35	0.03	0.77	−0.13
TOC	0.29	−0.02	0.30	0.85	0.36	0.78	0.31	−0.19	0.20	−0.08	0.00	0.88
< 16	0.24	0.52	0.16	0.74	0.28	0.82	0.11	0.20	0.02	0.60	0.32	0.65
< 63	0.15	0.43	0.17	0.79	0.24	0.86	0.10	0.02	−0.15	0.68	0.11	0.58
Var%	26.8	20.3	18.5	17.5	28.8	20.9	17.7	12.7	36.8	16.8	13.2	12.4
Cum%			83.1				80.1				79.2	

Components are rotated for the maximum variance. Loadings with values larger than 0.7 are marked in bold. Last two rows give the variance explained per component (Var%) and variance explained by all components (Cum%).

proxy for the amount of clay will lead to correlations between these radionuclides and dispersed contaminants that preferably adsorb to clay.

If the contamination is *localized* and thus cannot be considered dispersed the occurrence of correlations is less obvious, e.g. a large local discharge of pollutants that are rapidly immobilized by the sediment in the vicinity will usually not lead to correlations with natural radionuclides. Correlations may only be expected if one of the natural radionuclides is associated with the pollutant, e.g. uranium in waste releases from the fertilizer industry (Bolívar et al., 2002) or thorium in leachates from tailings from the tin industry (Hu et al., 1995).

An important prerequisite for the *dispersed* presence of a compound is that the compound should be mobile. The mobility of compounds in freshwater sediments is restricted by their adsorption to the sediments. In general, the distribution of a contaminant between the water compartment (C_w : concentration in water) and sediment (C_s : concentration on/in the sediment) is described by the sorption isotherm. For low concentrations these isotherms are often linear and described by $C_s = K_d C_w$. In this situation sorption can be quantified by the distribution coefficient K_d ($\text{m}^3 \text{kg}^{-1}$). Here we will discuss the mobility of the three natural radionuclides and of the anthropogenic radionuclide ¹³⁷Cs.

4.1.1. Uranium

Under standard environmental oxic conditions, uranium typically occurs in the hexavalent form as the aqueous uranyl ion (UO_2^{2+}). This ion is very mobile and via this

pathway uranium may be ‘redistributed’ over large areas. Uranium is known to accumulate in bioliths and especially the sorption of the uranyl ion to humic acids plays an important role (Szalay, 1964; Idiz et al., 1986). Uranyl may also adsorb to clays (montmorillonite, Catalano and Brown, 2005; illite, Seaman et al., 2001) through cation exchange. Adsorption of uranium is low at pH values less than 3, increases with increasing pH and reaches a plateau between pH 5 and 8, for higher pH adsorption decreases again. Typical values (EPA, 1999) for K_d ($\text{m}^3 \text{kg}^{-1}$) of uranium are 0.035 (sand), 0.4 (organic material), and 1.6 (clay).

4.1.2. Thorium

In an aquatic environment thorium is found only in tetravalent form and its solubility is limited by the formation of its almost insoluble hydroxide $\text{Th}(\text{OH})_4$ (Choppin, 2006). Moreover, Th (similar as PAH) has a very strong affinity towards suspended particles (Gustafsson et al., 1997) and if it becomes mobile it will be rapidly reabsorbed and immobilized.

4.1.3. Potassium

In nature ⁴⁰K is distributed as a monocharged positive ion and when in solution it is very mobile as almost all its salts are highly soluble. Both potassium and caesium are alkali metals and their chemical behaviour is similar. Consequently, in a freshwater environment potassium and caesium will compete for the same adsorption sites and both are expected to be primarily associated with clay minerals (Bhattacharyya, 1998).

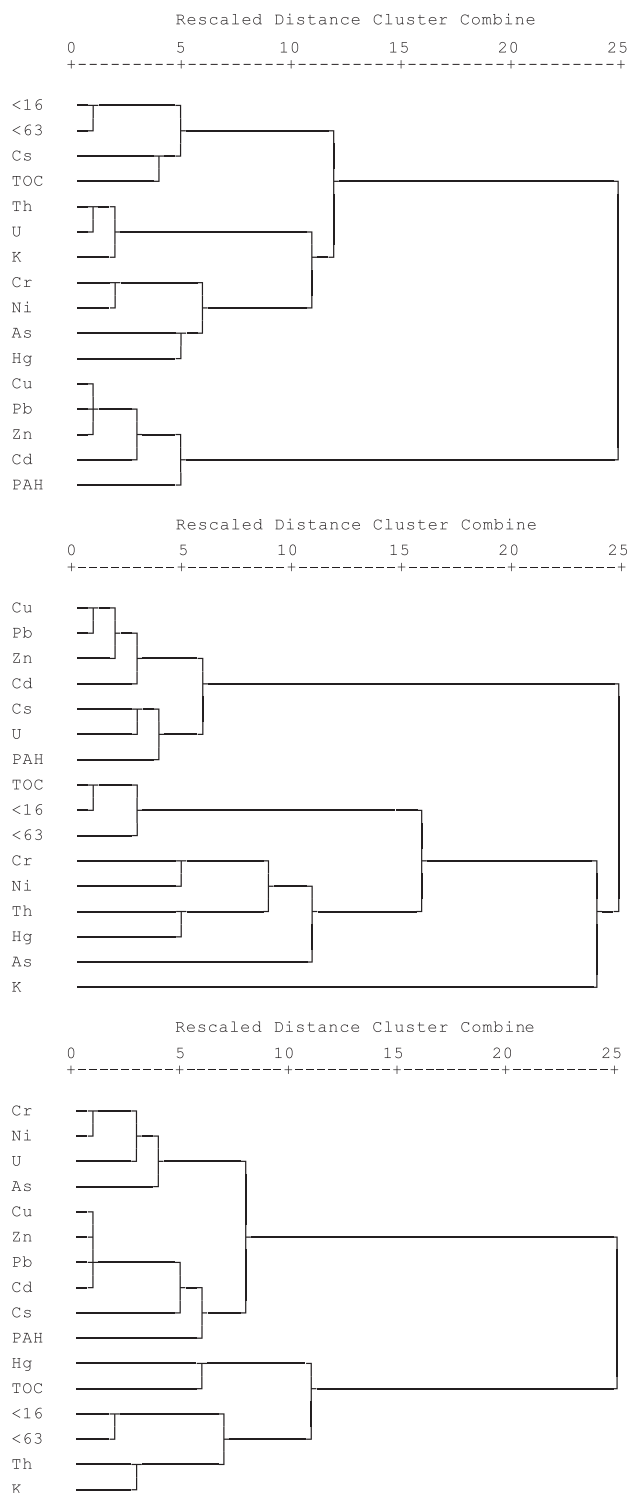


Fig. 6. Dendrograms of the cluster analysis of all data (top), Th < 20 data (middle) and Th > 20 data (bottom).

4.1.4. Caesium

In soils and sediments Cs occurs as a positive mono-charged ion. This ion is highly mobile in an aqueous environment due to its low hydration energy ($-276 \text{ kJ mole}^{-1}$, Shahwan et al., 2005). Clay minerals are especially effective in adsorbing Cs (Beneš et al., 1989).

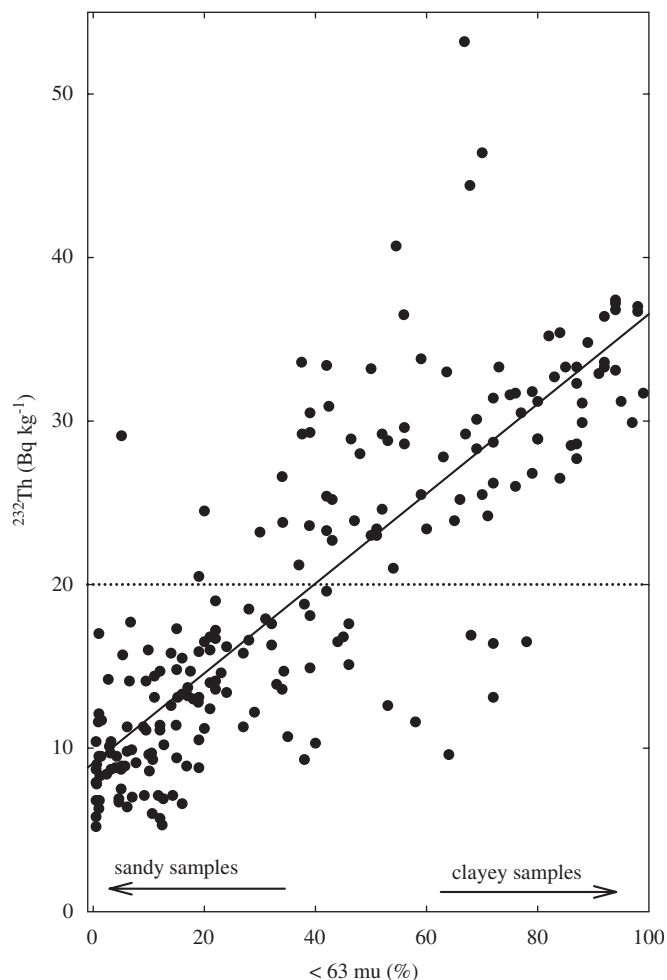


Fig. 7. ^{232}Th activity concentration (Bq kg^{-1}) as a function of the fraction of grain sizes $< 63 \mu\text{m}$. The dotted line represents the $\text{Th} = 20 \text{ Bq kg}^{-1}$ level at which the total data set has been split. The solid line is a least-squares fit to the total data set.

Table 8 lists K_d -values of Cs for some minerals that have a relevant presence in Dutch sediments. This table shows that indeed these K_d -values for clay minerals are much larger than for quartz indicating the relative importance of adsorption to clay with respect to adsorption to sand.

In general, illites adsorb more Cs than smectites but sometimes also high K_d values for smectites like vermiculite are reported (see Table 8). Adsorption of Cs to clay minerals is usually quite fast but slow sorption is observed on illite. Although the latter sorption has long been found as almost irreversible in laboratory studies (Comans and Hockley, 1992) recent research indicates that under more natural conditions reversible ion exchange occurs (De Koning and Comans, 2004). This seems to be more consistent with the ubiquity of Cs from Chernobyl in water and foodstuffs. Illites have highly specific sites at the frayed edges (exposed edges of the interlayers of the clay platelets; Öztóp and Shahwan, 2006) where a partial removal of K from the interlayers creates sites for Cs to enter the edges of the interlayer. Upon entering Cs sheds its hydration shell

Table 8
Distribution coefficients of Cs (at trace concentrations) on different minerals occurring in (Dutch) sediments

Mineral	K_d ($\text{m}^3 \text{kg}^{-1}$)
<i>Clay minerals</i>	
Kaolinite	0.9–2.5
Illite	0.4–12
Montmorillonite	1.1–25
Vermiculite	52–59
<i>Others</i>	
Mica	26–61
Quartz	0.06–0.1

Table based on data from: Cornell (1993), Kónya et al. (2005), and EPA (1999).

and forms polar bonds with structural oxygen atoms and so collapsing the edges. Cs is strongly held at these positions. For smectite clays like montmorillonites and vermiculites non-specific sorption sites are present at the surfaces and in the interlayers. These sites are filled by ion exchange processes and Cs is in competition for these sites with other cations in solution. The sorption to kaolinite is determined by the nature of its surface and the edges and is less specific than for the other clay minerals. Micas have a large sorption capacity for Cs but are only present in small percentages in the sand fraction of sediments. Quartz is not important as no larger K_d values than 0.1 are mentioned in literature (Cornell, 1993).

In conclusion, Cs in Dutch freshwater is very mobile but restricted by sorption on sediment and especially clay minerals in which most likely reversible adsorption to illites plays an important role. The sand fraction of the sediment is of minor importance. In case larger amounts of micas are present they may also contribute in immobilizing Cs. In general, Cs will be associated with the clay fraction and thus be concentrated in clayey samples. This is consistent with the finding that ^{137}Cs is also enhanced in the clayey samples (Table 4).

The correlation between K, U and Th for the complete data set is positive and moderate to strong (Fig. 5). Especially strong correlations are found between Th and U and between K and U with R^2 values larger than 0.8. This reflects the fact that the natural radionuclides are all more abundant in clayey samples with respect to sandy samples and so inducing correlations. The strength of these correlations is somewhat lower in the two subgroups as the scatter in the data has a relatively higher influence when the range of the data set is reduced.

Fig. 5 shows that U correlates well (and even better than the fraction $<63 \mu\text{m}$) with almost all metals and in particular with Pb, Ni, Zn, and Cu for all data and the two subgroups. Furthermore, U also correlates with Cr but this is linked to the subgroup with $\text{Th} > 20$ (clayey samples). The correlations of Cs with the metals show a similar but less pronounced pattern as for U.

From Fig. 5 it is also clear that Th and especially K do not correlate well with the metals. As Th and K are (similar as U) associated with the clay fraction this indicates that it is not simply the presence of the natural radionuclides *in* and the adsorption of the metals and Cs *to* the clay fraction that is the underlying cause of the correlations of U and Cs with the metals. Most likely also the mobility of the radionuclides is an important aspect. It has been pointed out earlier that U and Cs are very mobile in an aqueous environment and have a high affinity for clays. In addition to the structural presence of U in clays the adsorption of the dissolved uranyl ion to clay minerals will enhance the U content in clayey sediments and so strengthen correlations with metals that are also adsorbed on the clay minerals. Thorium, on the other hand, is much less mobile and ‘misses out on’ this process of concurrent sorption with the metals. Consequently, correlations between Th and the metals are less strong. In this context the lower degree of correlation (as compared to U) between Cs and the metals may be explained by the fact that these correlations completely depend on adsorption of both Cs and metals to the clay fraction as Cs is not structurally incorporated in clay minerals.

It is remarkable that correlations of K with the metals seem to be completely absent. It is speculated that the presence of potassium-feldspars (and maybe micas) might obscure the relation between K and clays. This effect has also been observed in radiometric characterization of sand and mud in the Rhine-Meuse estuary (Van Wijngaarden et al., 2002).

Adsorption of metals to clays is often studied from the viewpoint of using clay layers as linings to prevent leaching from waste deposits. Similar as for Cs (Table 8) clay minerals are found to be good sorbents for metals like Cd, Cr, Cu, Ni, Pb and Zn (Abollino et al., 2003). This adsorption decreases with decreasing pH and also in the presence of organic substances. In case of lower pH the hydrogen ion competes with the metals for adsorption sites while organic substances form complexes with the metal ions hindering adsorption to the clay. In general Pb is retained better than Cd (Barbier et al., 2000). Moreover, Covel et al. (2004) reported $\text{Pb} > \text{Cr} > \text{Cu} > \text{Cd} \approx \text{Ni} \approx \text{Zn}$ as the most common selectivity sequence for adsorption on soils with a high clay content. In sediments, under anoxic conditions, divalent cationic metals (Cd, Cu, Pb, Zn and Ni) will form metal sulphides. If the sulphide concentration is sufficiently high (as will be the case in most freshwater sediments) these metals will mainly be present as insoluble metal sulphides (Doig and Liber, 2006). In addition, under anoxic conditions as occur in the deeper sediments, uranium may be reduced to its immobile tetravalent state.

From this information it is concluded that indeed correlation between metals and of metals with U and Cs may be expected on basis of their common affinity for clay minerals. The strength of these correlations may be influenced by variations in pH and/or organic substances. Furthermore, in sediments under anoxic conditions

precipitation of metal sulphides together with reduction and subsequent immobilization of uranium might enhance correlations.

4.2. Principal components and cluster analysis

As the PCA and the CA resulted in a similar pattern of associations between the variables we will discuss them together. It appears that Pb, Zn, Cu and Cd are combined in one PC for all data and also for the two subgroups and moreover are also similar according to the CA. This most likely reflects their quite similar chemical behaviour as primarily positive divalent metals. However it is surprising that Ni (also primarily divalent) behaves differently and seems to be associated with Cr, this association is especially clear from the CA (Fig. 6). It is speculated that precipitation of metal sulphides may play a role in the formation of these associations. Metal sulphides are very insoluble and in freshwater sediments these sulphides will readily precipitate as in most instances the sulphide ion is present in sufficient amounts (Buykx et al., 2002). In general, metal sulphides will precipitate in order of decreasing solubility product, K_{sp} , defined as the product of the ion concentrations of the metal and sulphide. Although K_{sp} values are difficult to measure and reported values may vary over an order of magnitude or more it appears that NiS is more soluble than the other metal sulphides (Fig. 8). Consequently, Ni will be somewhat more mobile and in that way dissimilar from Pb, Zn Cu and Cd.

With respect to Cr we have to consider that Cr may exist in various valence states of which the Cr(III) and Cr(VI) states are the most stable (Saleh et al., 1989). In the Medusa project data base only total Cr concentration values are included and differentiation between these two states could not be made. From the literature it appears that in natural waters both valence states occur and that

the trivalent state is less soluble and therefore less mobile than the hexavalent state (Mattuck and Nikolaidis, 1996). Under environmental conditions Cr(III) exists as the insoluble chromium hydroxide whilst Cr(VI) is present as either the soluble chromate or monohydrogen chromate ion (Apte et al., 2006). Considering the close association of Cr and the relatively mobile Ni this might imply that the more mobile species Cr(VI) is the most prevalent in Dutch freshwater.

Another difference between Ni and Cr and the other metals is that their mean concentrations (Ni: 16.3 ppm; Cr: 32 ppm, Table 2) are significantly lower than their background value (Ni: 35 ppm; Cr: 32 ppm, Table 1). This may have resulted in a suppression of possible associations of Ni and Cr with the other metals because these associations are difficult to observe on the verge of the background levels.

Mercury and arsenic do not show significant association with the other metals. In case of Hg this is not expected as its sulphide is very insoluble (Fig. 8). However, Hg was only present in significant amounts in two of the 13 projects and it is suspected that these contaminations remained localized and so prohibiting possible correlations. Arsenic was present in almost all projects and for the clayey samples (Th>20) seems to follow Cr, U and Ni (Fig. 6, bottom) indicating As also remains relatively mobile in the sediment.

From the CA it appears there is some relation between PAH and the metals Cu, Zn, Pb and Cd. This is also reflected in the PCA except for the clayey samples (Th>20). This is rather surprising as PAH are hydrophobic compounds and in natural water are expected to remain sorbed to the sediment (Brion and Pelletier, 2005) and for these compounds sorption is dominated by that on/in the organic matter component of the sediment (Warren et al., 2003). This sorption process is more strongly governed by PAH removal from the water phase and partitioning into hydrophobic sites in the organic matter than by direct interactions with adsorbing surfaces. As fine clayey sediments will usually have a higher total organic content than sandy sediments and also have a higher surface to volume ratio, these fine sediments are expected to have a higher PAH content. Moreover, fine sediments will go readily in suspension in high flow zones and are deposited in low flow (accumulation) zones leading to a further enhancement of PAH in fine sediments. Consequently, in the clayey samples an association between TOC and PAH is expected. However, in our data set, correlations between PAH and TOC are low or non-significant and as mentioned above in the PCA and CA associations between PAH and the metals are found rather than between PAH and TOC.

A speculative way out of this paradox might be found in the age of the PAH contamination. Presently, due to strict emission reduction policy, in the Netherlands the freshwaters itself are relatively clean but the PAH contamination in the sediments stems from the past decades

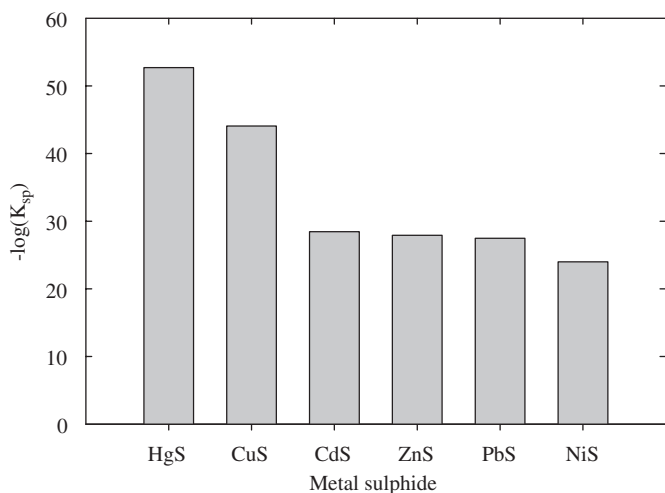


Fig. 8. Solubility products K_{sp} of divalent metal sulphides (data from Weast, 1972)

(Cornelissen et al., 1999). It has been proposed that after relatively fast partitioning into the organic matter PAH will become more strongly bound (sequestration process, Brion and Pelletier, 2005) to the sediment, e.g. trapped in clay meso- or micro-pores or after degradation being chemically bound to the inorganic matter (Oren and Chefetz, 2005). In aging contaminated sediments such a sequestration process will decrease the association of PAH with organic matter and induce a stronger association with micro-porous inorganic matter. For the aged PAH contamination in the Dutch sediments this might lead to PAH correlated with metals by a common association to the inorganic clay fraction in favour of the normally expected correlation of PAH with TOC.

5. Conclusions

After this discussion of the results of the PCA and CA we are now in the position to draw conclusions regarding the implications of these results for the two main objectives mentioned in the Introduction.

With respect to the first objective we conclude that for uranium and to a lesser extent caesium correlations exist with especially metals for all the Dutch freshwater represented by the Medusa database. However, it should be noted that although these correlations are moderate to strong for the combined data, often stronger and even unexpected correlations are found per project. An example is given in Fig. 9 for a project in the harbour of Deventer (The Netherlands). For this project a correlation between U and Pb is found that is stronger than for the whole dataset and, what is more, correlation is found between Cs and PAH that could be used for assessment of the distribution of the PAH contamination.

Regarding the second objective it is concluded that indeed the relative high natural content of U in clay in combination with the sorption properties of clay is an important factor in bringing about correlations with U. An

additional prerequisite for strengthening the correlations is that the radionuclide is also mobile. This appears to be the case for U and Cs but not for Th and K. For Cs and the metals their common affinity for clay is likely the governing mechanism for inducing correlations. In case of U it seems plausible that also anoxic conditions in sediments enhance correlations due to precipitation of metal sulphides and at the same time reduction and immobilization of U. For U this leads to correlations and associations with the metals that are stronger than those of the clay fraction (grain size $<63\ \mu\text{m}$) with the metals.

In summary, the goal of this study was to assess the correlations that have been found between contaminants and radionuclides during various projects in Dutch freshwater sediments. More specifically it was studied whether some correlations would be valid for the entire Dutch freshwater system. The assessment was based on a multivariate analysis of a database containing data on radionuclide content, sediment properties and concentrations of contaminants. It was found that indeed U and to a somewhat lesser degree Cs show correlations with especially the metals. For K and Th, except with the grain sizes, no pronounced correlations were found. It is likely that the higher mobility of U and Cs discriminates their behaviour from that of the other radionuclides. For Cs it appears that especially the preference of Cs and metals for adsorption to clay is the dominant factor leading to correlations. Correlations between U and metals seem to be controlled by a common affinity of U and the metals for the clay component in combination with clay having relatively high U contents. In addition, under the anoxic conditions in sediment the concurrent precipitation of metal sulphides and reduction and immobilization of U may lead to a stronger association between U and the metals. Moreover, this association is even closer than that of clay (grain size $<63\ \mu\text{m}$) with the metals. Due to these correlations spatial information of in situ measurements of gamma activity can be used as a proxy for sediment contamination.

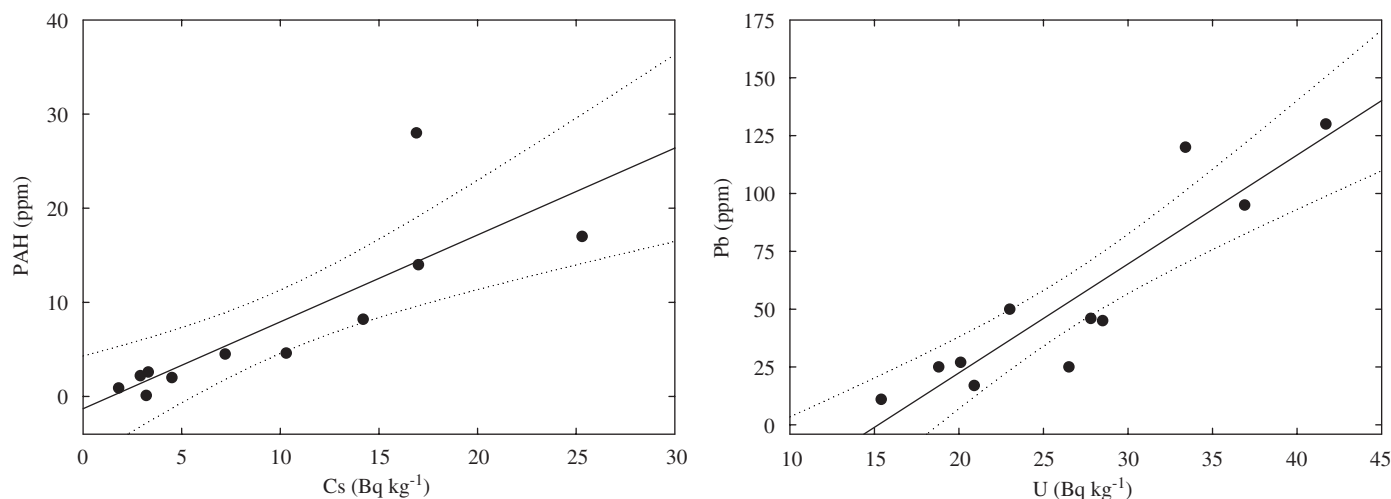


Fig. 9. Correlation plots from a project in the harbour of Deventer, the Netherlands. Solid lines are linear regressions: PAH (ppm) = $-1.3 + 0.9\ \text{Cs}$ (Bq kg⁻¹) ($R^2 = 0.70$) and Pb (ppm) = $-71.6 + 4.71\ \text{U}$ (Bq kg⁻¹) ($R^2 = 0.83$). Dotted lines are 95% confidence intervals.

Acknowledgement

This project was conducted with support of the Casimir programme of the Netherlands Organization for Scientific Research that aims at increasing the mobility of research staff in the public and private sectors.

References

- Abollino, O., Aceto, M., Malandrino, M., Sarzanini, C., Mentasti, E., 2003. Adsorption of heavy metals on Na-montmorillonite. Effect of pH and organic substances. *Water Res.* 37, 1619–1627.
- Apte, A.D., Tare, V., Bose, P., 2006. Extent of oxidation of Cr(III) to Cr(VI) under various conditions pertaining to the natural environment. *J. Hazard. Mater. B* 128, 164–174.
- Barbier, F., Duc, G., Petit-Ramel, M., 2000. Adsorption of lead and cadmium ions from aqueous solution to the montmorillonite/water interface. *Colloids Surf. A* 166, 153–159.
- Beneš, P., Lam Ramos, P., Poliak, R., 1989. Factors affecting interaction of radiocesium with freshwater solids. I. pH, composition of water and the solids. *J. Radioanal. Nucl. Chem.* 133, 359–376.
- Bhattacharyya, D.K., 1998. Issues in the disposal of waste containing naturally occurring radioactive material. *Appl. Radiat. Isot.* 49, 215–226.
- Bikit, I., Slivka, J., Vesković, M., Varga, E., Žikić-Todorović, N., Mrđa, D., Forkapić, S., 2006. Measurement of Danube sediment radioactivity in Serbia and Montenegro using gamma ray spectrometry. *Radiat. Meas.* 41, 477–481.
- Bolívar, J.P., García-Tenorio, R., Masa, J.L., Vaca, F., 2002. Radioactive impact in sediments from an estuarine system affected by industrial wastes releases. *Environ. Int.* 27, 639–645.
- Brion, D., Pelletier, E., 2005. Modelling PAHs adsorption and sequestration in freshwater and marine sediments. *Chemosphere* 61, 867–876.
- Buyx, S.E.J., Van den Hoop, M.A.G.T., Loch, J.P.G., 2002. Dissolution kinetics of heavy metals in Dutch carbonate–sulfide-rich freshwater sediments. *J. Environ. Qual.* 31, 573–580.
- Catalano, J.G., Brown, G.E., 2005. Uranyl adsorption onto montmorillonite: evaluation of binding sites and carbonate complexation. *Geochim. Cosmochim. Acta* 69, 2995–3005.
- Choppin, G.R., 2006. Actinide speciation in aquatic systems. *Mar. Chem.* 99, 83–92.
- Comans, R.N.J., Hockley, D.E., 1992. Kinetics of cesium sorption on illite. *Geochim. Cosmochim. Acta* 56, 1157–1164.
- Cornelissen, G., Van Zuilen, H., Van Noort, P.C.M., 1999. Particle size dependence of slow desorption of in situ PAHs from sediments. *Chemosphere* 38, 2369–2380.
- Cornell, R.M., 1993. Adsorption of cesium on minerals: a review. *J. Radioanal. Nucl. Chem.* 171, 483–500.
- Covelo, E.F., Andrade, M.L., Vega, F.A., 2004. Heavy metals adsorption by humic umbrilsols: selectivity sequences and competitive sorption kinetics. *J. Colloid Interface Sci.* 280, 1–8.
- De Koning, A., Comans, R.N.J., 2004. Reversibility of radiocaesium sorption on illite. *Geochim. Cosmochim. Acta* 68, 2815–2823.
- De Meijer, R.J., Limburg, J., Venema, L.B., 2002. Natural radioactivity in monitoring waste disposals. *Phys. Scr.* T97, 139–147.
- Doig, L.E., Liber, K., 2006. Nickel partitioning in formulated and natural freshwater sediments. *Chemosphere* 62, 968–979.
- Dyrstad, K., 1998. Selective improvements in multiquality products assisted by rotated principal components. *Chemometr. Intell. Lab. Syst.* 42, 115–124.
- EPA, 1999. Understanding Variation in Partition Coefficient, K_d , Values, vol. II: Review of Geochemistry and Available K_d Values for Cadmium, cesium, Chromium, Lead, Plutonium, Radon, Strontium, Thorium, Tritium (3H), and Uranium. EPA Report 402-R-99-004B, United STATES Environmental Protection Agency, Office of Air and Radiation, USA.
- Golobočanin, D., Škrbić, B.D., Miljević, N.R., 2004. Principal component analysis for soil contamination with PAHs. *Chemometr. Intell. Lab. Syst.* 72, 219–223.
- Gustafsson, Ö., Gschwend, P.M., Buesseler, K.O., 1997. Using ^{234}Th disequilibria to estimate the vertical removal rates of polycyclic aromatic hydrocarbons from the surface ocean. *Mar. Chem.* 57, 11–23.
- Hendriks, P.H.G.M., Limburg, J., De Meijer, R.J., 2001. Full-spectrum analysis of natural γ -ray spectra. *J. Environ. Radioact.* 53, 365–380.
- Hu, S.J., Kandaiya, S., Lee, T.S., 1995. Studies of the radioactivity of Amang effluent. *Appl. Radiat. Isot.* 46, 147–148.
- Idiz, E.F., Carlisle, D., Kaplan, I.R., 1986. Interaction between organic matter and trace metals in a uranium rich bog, Kern County, California, USA. *Appl. Geochem.* 1, 573–590.
- Kelderman, P., Drossaert, W.M.E., Min, Z., Galione, L.S., Okonkwo, L.C., Clarisse, I.A., 2000. Pollution assessment of the canal sediments in the city of Delft (The Netherlands). *Water Res.* 34, 936–944.
- Kónya, J., Nagy, N.M., Nemes, Z., 2005. The effect of mineral composition on the sorption of cesium ions on geological formation. *J. Colloid Interface Sci.* 290, 350–356.
- Koomans, R.L., Limburg, J., 2005. In situ mapping of heavy metal concentrations and organic micro compounds. In: Proceedings of the Third International Conference on Remediation of Contaminated Sediments, Venice, 2005. Batelle Press, Columbus, USA.
- Lahr, J., Maas-Diepeveen, J.L., Stuijzand, S.C., Leonards, P.E.G., Drüke, J.M., Lücker, S., Espeldoorn, A., Kerkum, L.C.M., van Stee, L.L.P., Hendriks, A.J., 2003. Responses in sediment bioassays used in the Netherlands: can observed toxicity be explained by routinely monitored priority pollutants? *Water Res.* 37, 1691–1710.
- Lee, C.S.-l., Li, X., Shi, W., Cheung, S.C.-n., Thornton, I., 2006. Metal contamination in urban, suburban, and country park soils of Hong Kong: a study based on GIS and multivariate statistics. *Sci. Total Environ.* 356, 45–61.
- Locher, W.P., De Bakker, H., 1990. *Bodemkunde van Nederland. Deel 1: Algemene Bodemkunde.* Malmberg Den Bosch, The Netherlands.
- Mattuck, R., Nikolaidis, N.P., 1996. Chromium mobility in freshwater wetlands. *J. Contam. Hydrol.* 23, 213–232.
- Meloun, M., Sánka, M., Němec, P., Křitková, S., Kupka, K., 2005. The analysis of soil cores polluted with certain metals using the Box–Cox transformation. *Environ. Pollut.* 137, 273–280.
- Miller, J.N., Miller, J.C., 2005. *Statistics and Chemometrics for Analytical Chemistry.* Pearson Prentice-Hall, Harlow, England.
- MNP, 2006. Milieu en Natuur Planbureau, Milieucompendium, <<http://www.mnp.nl/>>.
- Mohanty, A.K., Sengupta, D., Das, S.K., Vijayan, V., Saha, S.K., 2004. Natural radioactivity in the newly discovered high background radiation area on the eastern coast of Orissa, India. *Radiat. Meas.* 38, 153–165.
- NW4, 1999. Vierde Nota Waterhuishouding (NW4), Dutch Ministry of Transport, Public Works and Water Management.
- Oren, A., Chefetz, B., 2005. Sorption–desorption behavior of polycyclic aromatic hydrocarbons in upstream and downstream river sediments. *Chemosphere* 61, 19–29.
- Öztop, B., Shahwan, T., 2006. Modification of a montmorillonite–illite clay using alkaline hydrothermal treatment and its application for the removal of aqueous Cs^+ ions. *J. Colloid Interface Sci.* 295, 303–309.
- Reimann, C., Filzmoser, P., 1999. Normal and lognormal data distribution in geochemistry: death of a myth. Consequences for the statistical treatment of geochemical and environmental data. *Environ. Geol.* 39, 1001–1014.
- Römkens, P.F.A.M., Bonten, L.T.C., Rietstra, R.P.J.J., Groenenberg, J.E., Plette, A.C.C., Bril, J., 2003. Uitspoeling van zware metalen uit landbouwgronden. Alterra-Report 791, Alterra, Wageningen, The Netherlands.
- Saleh, F.Y., Parkerton, T.F., Lewis, R.V., Huang, J.H., Dickson, K.L., 1989. Kinetics of chromium transformations in the environment. *Sci. Total Environ.* 86, 25–41.

- Seaman, J.C., Meehan, T., Bertsch, P.M., 2001. Immobilization of cesium-137 and uranium in contaminated sediments using soil amendments. *J. Environ. Qual.* 30, 1206–1213.
- Sena, M.M., Frighetto, R.T.S., Valarini, P.J., Tokeshi, H., Poppi, R.J., 2002. Discrimination of management effects on soil parameters by using principal components analysis: a multivariate analysis case study. *Soil Till. Res.* 67, 171–181.
- Shahwan, T., Akar, D., Eroğlu, A.E., 2005. Physicochemical characterization of the retardation of aqueous Cs^+ ions by natural kaolinite and clinoptilolite minerals. *J. Colloid Interface Sci.* 285, 9–17.
- Struijs, J., Ritsema, R., Van der Kamp, R., De Zwart, D., 2000. A pilot of new monitoring techniques. RIVM Report 607200 003. RIVM, Bilthoven, The Netherlands.
- Szalay, A., 1964. Cation exchange properties of humic acids and their importance in the geochemical enrichment of UO_2^{++} and other cations. *Geochim. Cosmochim. Acta* 28, 1605–1614.
- Van den Berg, G.A., Loch, J.P.G., Van der Heijdt, L.M., Zwolsman, J.J.G., 1999. Mobilisation of heavy metals in contaminated sediments in the River Meuse, The Netherlands. *Water Air Pollut.* 116, 567–586.
- Van Wijngaarden, M., Venema, L.B., De Meijer, R.J., Zwolsman, J.J.G., Van Os, B., Gieske, J.M.J., 2002. Radiometric sand–mud characterisation in the Rhine-Meuse estuary. Part A. Fingerprinting. *Geomorphology* 43, 87–101.
- Venema, L.B., De Meijer, R.J., 2001. Natural radionuclides as tracers of the dispersal of dredge spoil dumped at sea. *J. Environ. Radioact.* 55, 221–239.
- Warren, N., Allen, I.J., Carter, J.E., House, W.A., Parker, A., 2003. Pesticides and other micro-organic contaminants in freshwater sedimentary environments—a review. *Appl. Geochem.* 18, 159–194.
- Weast, R.C., 1972. *Handbook of Chemistry and Physics*, 53rd ed., 1972–1973. CRC Press, Cleveland, USA.
- Winkels, H.J., Blom, G., Kroonenberg, S.B., Lijklema, L., 1998. Dilution of riverine heavy metal input concentration by suspension of sediments and algal growth in the IJsselmeer. *Water Res.* 32, 2931–2940.
- Zhu, M., Ghodsi, A., 2006. Automatic dimensionality selection from the scree plot via the use of profile likelihood. *Comput. Stat. Data An.* 51, 918–930.